

We are IntechOpen, the world's leading publisher of Open Access books Built by scientists, for scientists

6,900

Open access books available

186,000

International authors and editors

200M

Downloads

Our authors are among the

154

Countries delivered to

TOP 1%

most cited scientists

12.2%

Contributors from top 500 universities



WEB OF SCIENCE™

Selection of our books indexed in the Book Citation Index
in Web of Science™ Core Collection (BKCI)

Interested in publishing with us?
Contact book.department@intechopen.com

Numbers displayed above are based on latest data collected.
For more information visit www.intechopen.com



Epitaxial Growth of Ge on Si by Magnetron Sputtering

Ziheng Liu, Xiaojing Hao, Anita Ho-Baillie and
Martin A. Green

Additional information is available at the end of the chapter

<http://dx.doi.org/10.5772/intechopen.73554>

Abstract

Epitaxial growth of Ge on Si has received considerable attention for its compatibility with Si process flow and the scarcity of Ge compared with Si. Applications that drive the efforts for integrating Ge with Si include high mobility channel in metal-oxide-semiconductor field-effect transistors, infrared photodetector in Si-based optical devices, and template for III-V growth to fabricate high-efficiency solar cells. Epitaxy Ge on Si can be used as a virtual Ge substrate for fabrication of III-V solar cells, which has advantages of superior mechanical properties and low cost over Ge wafers. This work investigates the epitaxial growth of Ge on Si using magnetron sputtering, which is an environment-friendly, inexpensive, high throughput, and simple deposition technique. The effects of substrate temperature on the properties of Ge are analyzed. A novel method to epitaxially grow Ge on Si by magnetron sputtering at low temperature is developed using one-step aluminum-assisted crystallization. By applying an *in-situ* low temperature (50–150°C) heat treatment in between Al and Ge sputter depositions, the epitaxial growth of Ge on Si is achieved. This method significantly lowers the required temperature for and therefore the cost of epitaxial growth of Ge on Si.

Keywords: germanium, epitaxy, silicon, magnetron sputtering, substrate temperature, one-step aluminum-assisted crystallization

1. Introduction

Epitaxial growth of Ge on Si has received considerable attention for its compatibility with Si process flow and the scarcity of Ge compared with Si. Applications driving the efforts for integrating Ge with Si include: high mobility channel in metal-oxide-semiconductor field-effect transistors [1], infrared photodetector in Si-based optical devices [2], and template for III-V growth to fabricate high efficiency solar cells [3].

Ge wafers are the commonly used substrates for the fabrication of high efficiency III-V tandem solar cells [4–6]. Though cheaper than III-V materials, Ge wafers are over 100 times more expensive than Si accounting for more than 50% of the cell cost [3]. Compared with Ge wafer, Si wafer is an alternative with low cost, superior mechanical properties, and higher band gap more desirable for the bottom cell in a double or triple stack [7]. However, the lattice constant of Si is too small to match that of the III-V materials as shown in **Figure 1**. The lattice mismatch can induce large densities of defects negating the advantages of Si substrate. Several approaches have been investigated to control the defect density in this mismatched heterostructure including the insertion of various III-V intermediate layers, strained layer super-lattices, and the use of thermal annealing [8]. The obtained material qualities through these methods are not high enough to yield high efficiency III-V cells. A promising alternative is growing a Ge buffer layer to engineer the lattice constant of substrate surface to match that of III-V materials. Ge epitaxial film on Si can be used as a “virtual Ge substrate” for III-V solar cells. The virtual Ge substrate has advantages of superior mechanical properties and low cost over Ge wafer.

This work investigates the epitaxial growth of Ge on Si by magnetron sputtering, which is an environment-friendly, economical, high throughput, and simple deposition technique. Molecular beam epitaxy (MBE) and chemical vapor deposition (CVD) are widely used for Ge epitaxial growth on Si [10–13]. The MBE and CVD systems require higher vacuum (5×10^{-11} and 1.5×10^{-9} mbar, respectively) than magnetron sputtering (5×10^{-7} mbar) used in this work [14]. While MBE is the most expensive of the three and toxic gases such as germane and silane are used in a CVD system, magnetron sputtering offers a lower cost and safer alternative in

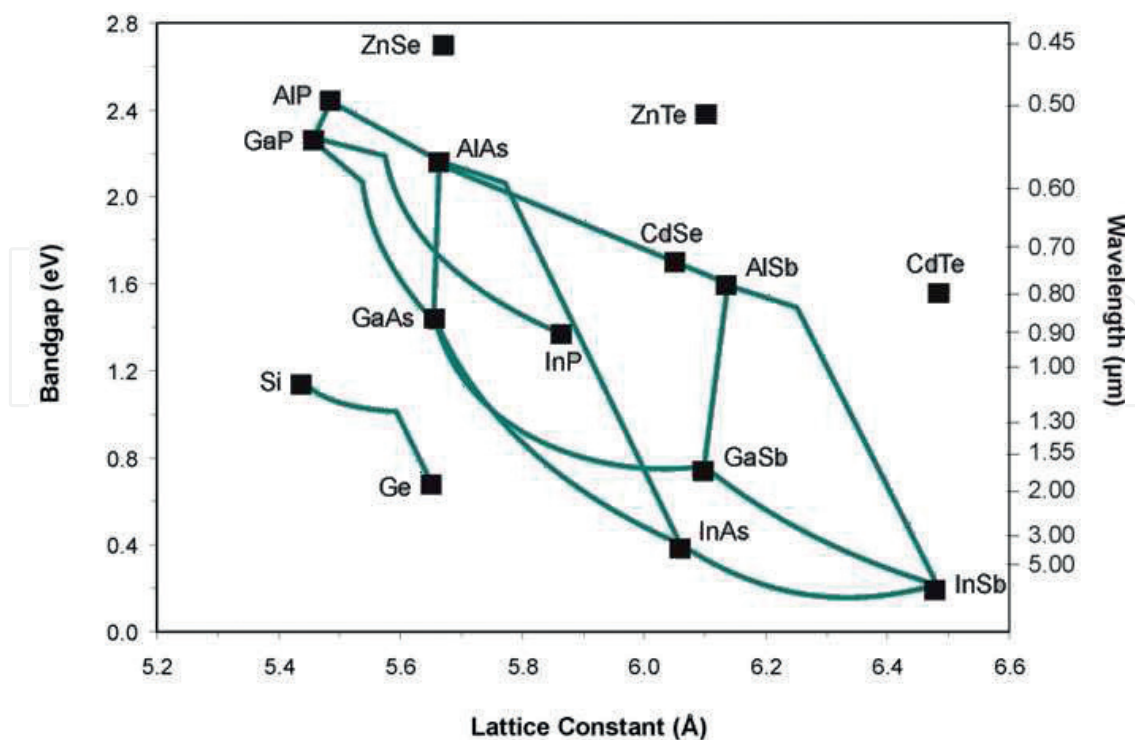


Figure 1. Lattice/band gap diagram for tetrahedrally coordinated semiconductors and their alloys [9].

supplying epitaxial Ge films on Si, which is potentially capable of large-scale production with good uniformity. This chapter presents the successful epitaxial growth of Ge on Si by magnetron sputtering, investigation on the effects of substrate temperature, and the development of a novel method to grow epitaxial Ge on Si by magnetron sputtering at low temperature through one-step aluminum-assisted crystallization.

2. Growth mechanism of Ge epitaxy on Si

2.1. Stranski-Krastanow growth

Three modes are possible in epitaxial growth: Frank-van der Merwe [15], Volmer-Weber [16], and Stranski-Krastanow [17], as shown in **Figure 2**. Frank-van der Merwe and Volmer-Weber modes are pure 2D layer-by-layer growth and 3D island growth, respectively. Stranski-Krastanow (SK mode) is a unique mode of 2D growth plus 3D island formation.

The interfacial free energy and the lattice mismatch determine which growth mode will be adopted in a given system [18]. In lattice-matched systems, the epitaxial film grows either in layer-by-layer mode or island growth mode depending on the interface energy and surface energy of the epitaxial film. In systems with large lattice mismatch, the growth mode may transit from 2D to island growth (SK mode) to relax strain in the epitaxial film. The early stage of the growth could be layer-by-layer due to the small interface energy. With epitaxial film growing thicker, strain energy is accumulated. The island formation is triggered to lower the total energy by introducing misfit dislocations.

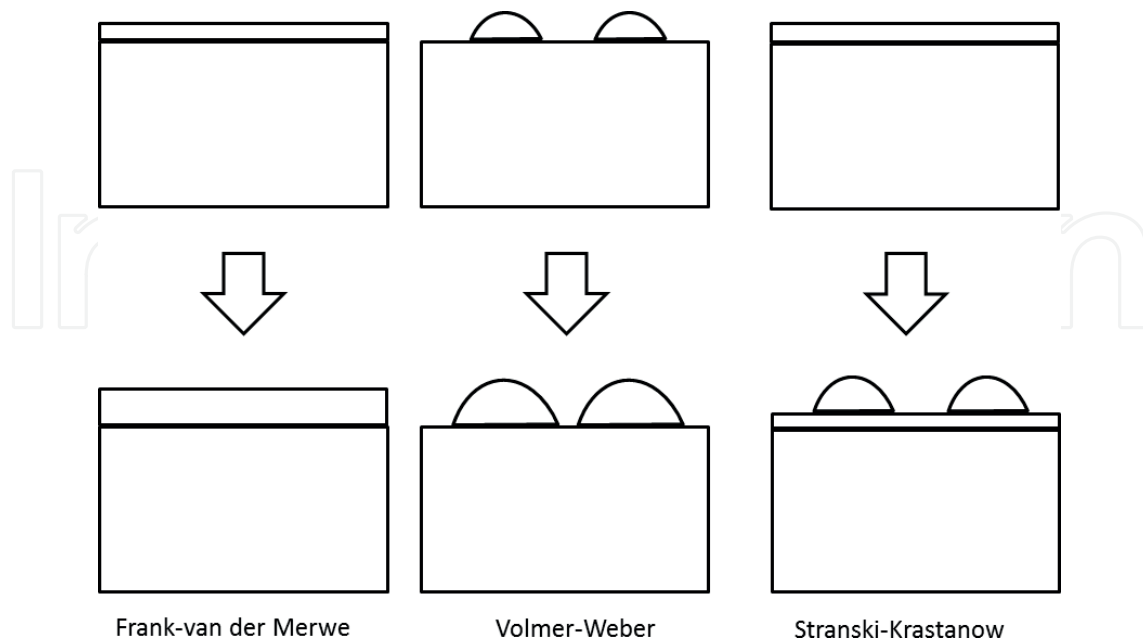


Figure 2. Illustrations of three possible epitaxial growth modes: Frank-van der Merwe, Volmer-Weber, and Stranski-Krastanow [18].

The Ge epitaxial growth on Si can be described as SK growth mode due to the 4.2% lattice mismatch between Si and Ge [19, 20]. In order to be used as a virtual substrate for the III-V deposition, smooth Ge surface is required [21, 22]. The island formation kinetics can be suppressed by shortened atomic surface migration length [23]. The reduced diffusion length can forbid the mass transport over a certain distance, which is required to form islands.

The diffusion length of Ge atoms could be reduced by using surfactant [24, 25] or low growth temperature [26, 27]. Sb has been used as a surfactant to suppress the Ge island formation. The energy barrier to diffuse is higher on the surfactant-covered surface than that of pure Si surface. In addition, the Ge atoms may be incorporated below the surfactant layer due to the site exchange process and therefore it is difficult for the Ge on top of the surfactant layer to diffuse as a relatively high diffusion barrier that has to be overcome. However, the use of surfactant also induces the incorporation of Sb leading to a n-type doping in the Ge film [28]. The effect of substrate temperature on the Ge surface roughness will be investigated in this work.

2.2. Lattice mismatch

Due to the 4.2% lattice mismatch between Si and Ge, the Ge epitaxial growth on Si is defect-free only below the critical thickness. The thin wetting layer is compressively strained in plane to adapt its lattice constant to that of the underlying Si substrate. In the meanwhile, a tensile strain is introduced in perpendicular inducing a tetragonal distortion to the Ge lattice. The biaxial strain compensates the lattice mismatch and therefore no defect is formed. The critical thickness for the defect-free growth of strained Ge on Si is in the range of several nanometers, which is also affected by the growth temperature [29].

When Ge growing above the critical thickness, misfit dislocations will nucleate at the interface and thread segments of dislocations run through the layer to the surface as threading dislocations. The misfit dislocations are incorporated to relax the strain arising from the lattice mismatch between Si and Ge by introducing extra half plane of atoms [30]. The misfit dislocations are energetically stable at the Si and Ge interface when Ge layer is above the critical thickness. As byproduct of misfit dislocations, threading dislocations thread either form a dislocation loop or terminate at the film surface. The threading dislocations are detrimental for the electrical devices because they lie across the whole film reducing the carrier mobility, carrier lifetime, and device reliability [31]. In this work, the epitaxial Ge layer has to be above the critical thickness to achieve a fully relaxed Ge surface matching the lattice of overlying III-V materials. The effect of substrate temperature on the threading dislocation density (TDD) of Ge will be investigated.

3. Epitaxial growth of Ge on Si by magnetron sputtering

3.1. Magnetron sputtering

Sputtering is a physical vapor deposition method. The target and the substrate are put on the cathode and anode, respectively. An inert gas such as argon (Ar) is introduced to create gaseous plasma by applying a voltage between the cathode and anode. The produced ions (Ar^+)

are accelerated toward the source target to sputter neutral atoms of the target. The ejected neutral atoms will travel to the substrate in a straight line unless they have collision with particles such as Ar atoms. The sputtered atoms, which arrive at the substrate may implant, bounce, diffuse, or simply stick onto the substrate, depending on their kinetic energies. As a result, the substrate will be coated by a thin film composed of target materials.

In conventional RF sputtering, most electrons lose their energy in nonionizing collisions are collected by the anode. The efficiency of ionization from energetic collisions between the electrons and gas atoms is low. Magnets are used to increase the percentage of electrons that participate in the ionization process. Large magnets are formed behind the target by applying a magnetic field at right angles to the electric field. The electrons are trapped near the target surface and kept in spiral motion until they collide with gas atoms. The increased probability of ionization significantly improves the efficiency of target materials sputtering and therefore increases the deposition rate at the substrate. Moreover, this allows the use of lower gas pressure, which may improve the film quality.

Figure 3 shows a schematic diagram of the RF magnetron sputtering system employed in this work. Four-inch intrinsic Ge target was used for the depositions of Ge film on Si and 4-inch SiO₂ target was used for capping layer deposition. The RF powers were supplied to the Ge and SiO₂ targets by two independent RF generators. The RF reverse power was reduced to zero by tuning the variable capacitors in the impedance matching network. Each target had a shutter to isolate the substrate from the plasma. The tilt angle of the targets and the distance between the targets and the substrate could be adjusted to achieve good uniformity.

Gas inlet with mass flow meter was used to supply argon into the main chamber. The vacuum in the main chamber was established by a mechanical rotary pump and a turbo molecular pump. Moreover, a load lock chamber was employed to protect the vacuum condition in the main chamber. Quartz halogen lamps were used to heat the substrate. The deposition rate was controlled by varying the RF power applied on the target and measured by a crystal monitor. The substrate was rotated during deposition to improve uniformity of the films.

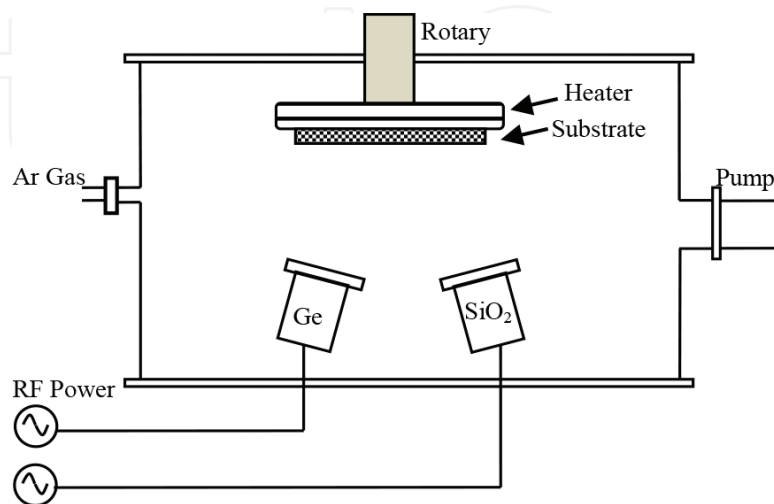


Figure 3. Schematic diagram of RF magnetron sputtering system used in this work.

3.2. Experimental details

In this work, the epitaxial growth of Ge on Si is demonstrated by sputtering Ge target using the AJA ATC-2200 magnetron sputtering system. The base pressure of the chamber was 5×10^{-7} mbar. N-type Si (100) wafers were used as the substrates. The Si substrates were cleaned using RCA solutions [32] followed by a HF dip. The Si substrate was immediately loaded into a load lock chamber after cleaning to minimize the oxidation of the Si surface.

The Ge films were sputter-deposited from a 4-inch intrinsic Ge target (99.999% purity) at a process pressure of 1.5×10^{-3} mbar. Rotation of 30 revolutions per minute was applied to the substrate during deposition to ensure the uniformity of the films. The Ar flow was kept at 15 sccm and the RF power applied to the Ge target was 150 W. The Ge deposition rate was 5 nm/min examined by a quartz crystal deposition rate monitor. 300 nm thick Ge films were sputter-deposited on Si at various substrate temperatures of 300, 400, and 500°C to investigate the effects of substrate temperature. The temperature calibration data was supplied and measured with a Si wafer by the manufacturer of the sputter system.

The surface morphology of Ge films was examined by atomic force microscopy (AFM) with Bruker Icon using the tapping mode. The scan area was $2 \times 2 \mu\text{m}$. The crystalline quality of the annealed Ge films was analyzed by high resolution X-ray diffraction (XRD), Raman spectroscopy, and transmission electron microscopy (TEM). The XRD measurements were performed with Bruker D8 at a voltage of 45 kV and a current of 100 mA, using $\text{Cu } K_{\alpha 1}$ radiation ($\lambda = 1.5406 \text{ \AA}$). The diffractometer was calibrated by making the Si (400) diffraction peak from the substrate maximized and at its theoretical position. Raman spectra of the Ge films were measured with Renishaw inVia Raman microscope using Ar^+ laser with wavelength of 514 nm as the excitation source. The beam power was limited to 6 mW to prevent the locally induced crystallization of Ge films during the measurement. Static mode with 20 times accumulation was employed to improve the signal to noise ratio. TEM measurements were conducted with Phillips CM200 microscope operating at 200 kV. The TEM samples were prepared by focused ion beam milling using Nova Nanolab 200.

3.3. Results and discussions

XRD 2θ - Ω scans were conducted on the Ge films deposited on Si at 300, 400, and 500°C in the 2θ range between 20 and 75° to examine the crystallinity of the Ge films. As shown in **Figure 4(a)**, apart from the strong Si (400) peak at 69.2° attributed to the substrate, only one peak at around 66° is observed which corresponds to Ge (400). The absence of any other Ge peaks indicates the Ge films might be single-crystalline Ge (100) which requires further examination by XRD Phi scans. **Figure 4(b)** shows Si (220) and Ge (220) Phi scan patterns collected from the sample deposited at 300°C by rotating the specimen with respect to the [110] axis. Only the four (220) reflections are observed in the Ge Phi scan pattern suggesting the film is with fourfold symmetry about an axis normal to the substrate [33]. In addition, the Ge (220) reflections align with the Si substrate (220) reflections indicating the Ge is single-crystalline epitaxy film.

The interface of the Ge film and Si substrate is investigated by high-resolution TEM to confirm the epitaxial growth of Ge on Si. As shown in the atomic-resolution image at the interface in

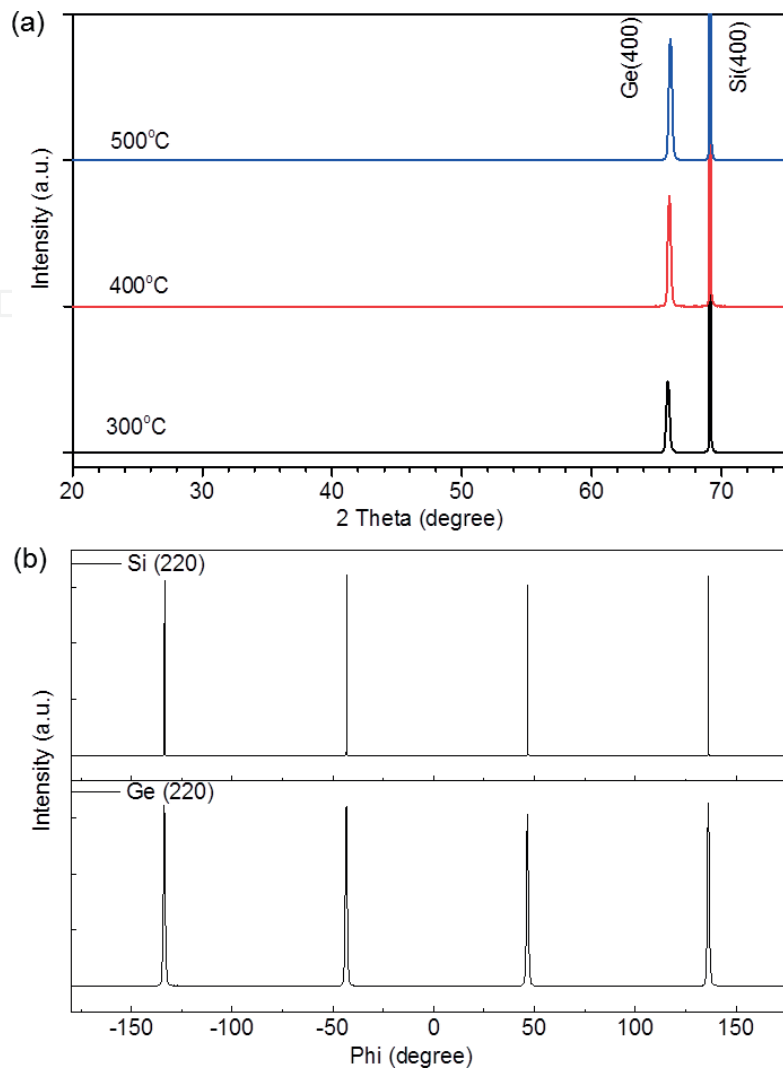


Figure 4. (a) XRD 2θ - Ω diffraction patterns of the Ge films deposited on Si at 300°C, 400°C, and 500°C, (b) Si (220) and Ge (220) phi scan patterns collected from the sample deposited at 300°C showing the epitaxial relationship between the Ge film and Si substrate.

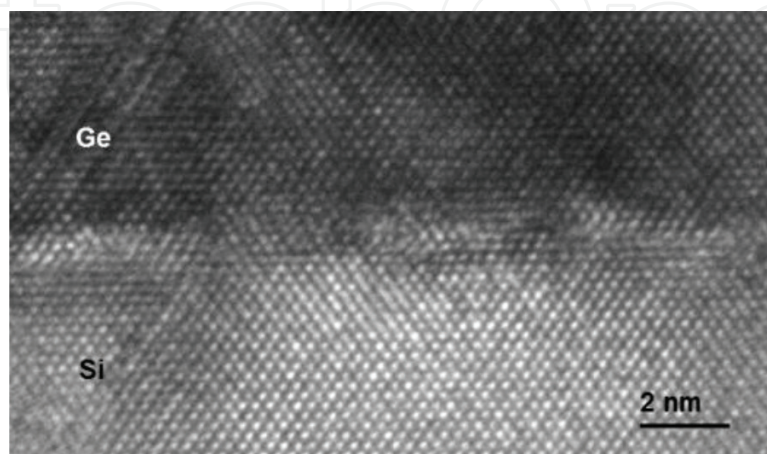


Figure 5. Atomic-resolution cross-sectional TEM image of Ge/Si interface on the sample deposited at 300°C.

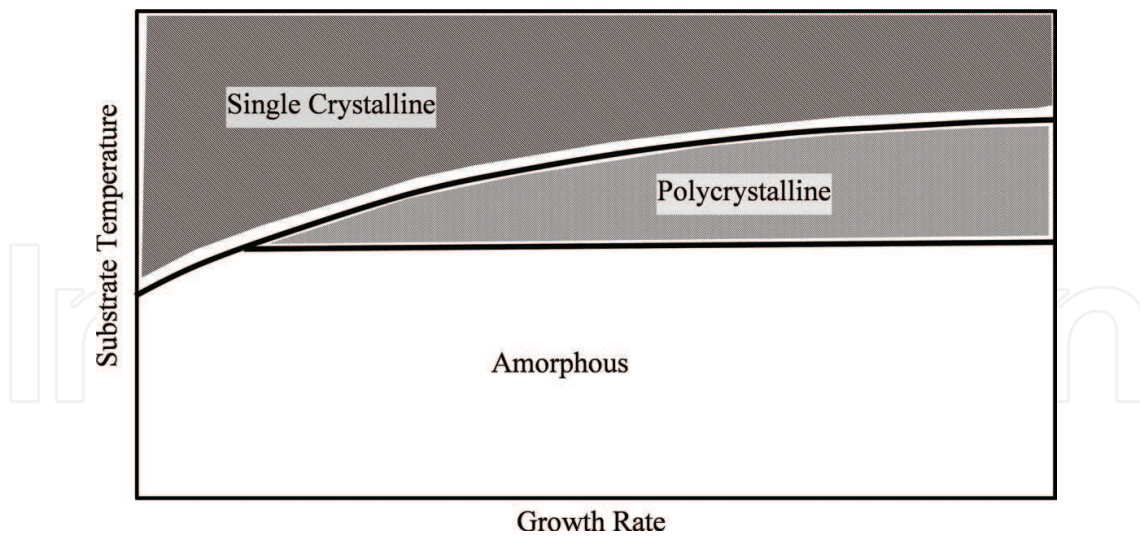


Figure 6. A schematic phase map of the crystallinity of as-deposited semiconductor films as function of growth rate and temperature [34].

Figure 5, the atoms are continuously aligned from the Si substrate to the grown Ge film suggesting successful epitaxy. This results is in good agreement with the XRD measurements.

The crystallinity of the as-deposited film depends on both the substrate temperature and growth rate as indicated in the schematic diagram shown in **Figure 6** [34]. The crystallinity can be improved by increasing the substrate temperature and reducing the growth rate. The XRD and TEM results suggest that substrate temperature of 300°C is enough to obtain single-crystalline Ge epitaxial growth on Si at the growth rate of 5 nm/min. The effects of substrate temperature on the quality of Ge films are investigated in the following section.

4. Effects of substrate temperature

As reviewed in the previous section, the substrate temperature may play an important role in determining the growth mode. The effects of substrate temperature on the properties of sputter-deposited epitaxial Ge films are discussed in this section. 300 nm thick Ge films were sputter-deposited on Si at various substrate temperatures of 300, 400, and 500°C.

The effect of substrate temperature on surface morphology of the Ge films is investigated using tapping mode AFM. **Figure 7** shows the 2D and 3D AFM images of the Ge films deposited at (a) 300°C, (b) 400°C, and (c) 500°C. It can be seen from the 3D AFM images that the surface morphology varies significantly among the Ge films deposited at different temperatures. The root mean square (RMS) surface roughness of the Ge films increases from 0.49 to 6.87 nm with substrate temperature increasing from 300 to 500°C. The increase in surface roughness with increasing substrate temperature indicates the growth switching from layer-by-layer mode to islanding mode with increasing substrate temperature.

In general, the epitaxial growth of Ge on Si follows the Stranski-Krastanow mode due to the lattice mismatch [18]. The growth initially follows layer-by-layer mode and progresses into island

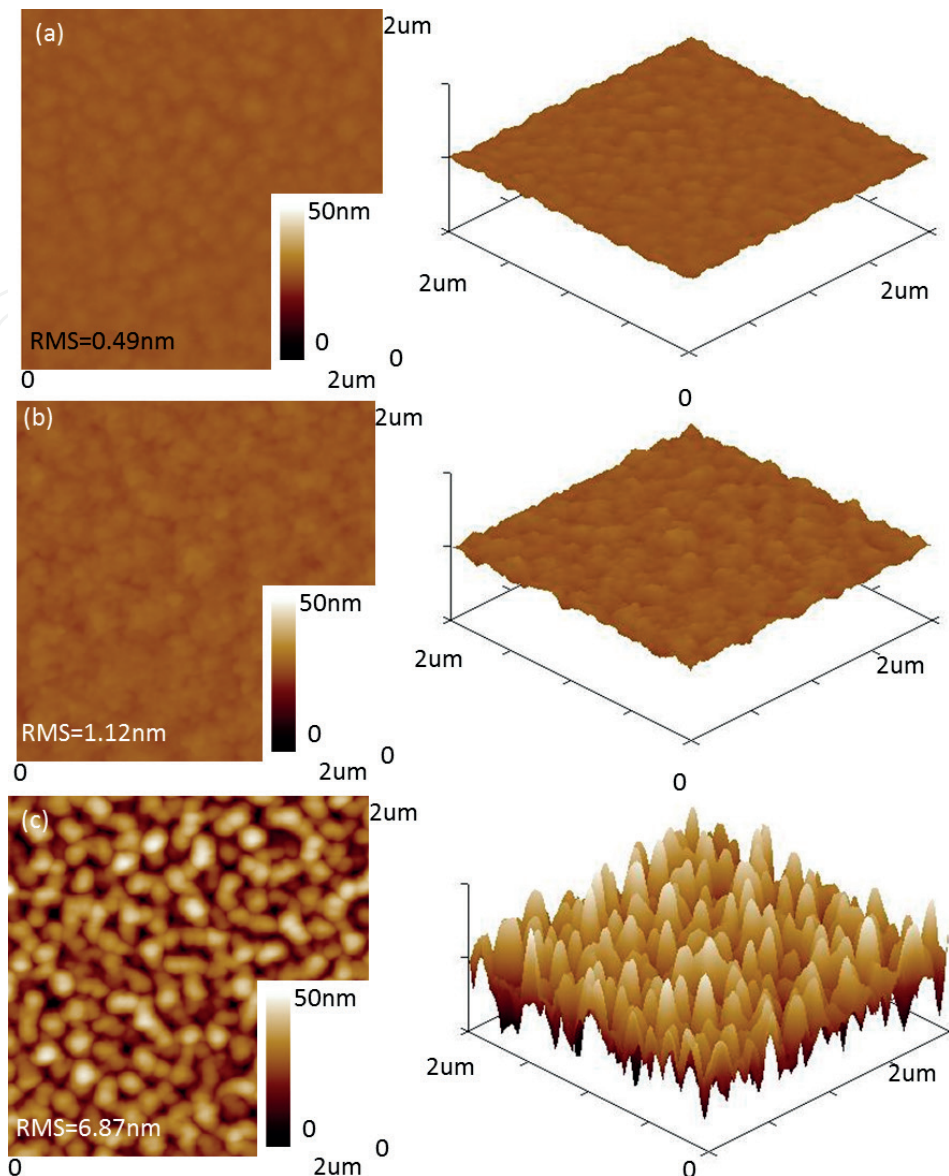


Figure 7. 2D and 3D AFM images showing the surface morphology of the Ge films deposited at (a) 300°C, (b) 400°C, and (c) 500°C.

mode when the layer becoming thicker. The thicker layer has large strain energy, which can be lowered by forming isolated thick islands. The island formation can be avoided by reducing the diffusion length of Ge. The reduced diffusion length hinders the mass transport of Ge over large distances which is necessary for the formation of islands [23]. Since the diffusion length of Ge decreases with reducing substrate temperature, the islanding is suppressed at low substrate temperature. As shown in **Figure 7**, layer-by-layer growth can be obtained at low temperature of 300°C to achieve smooth Ge surface, which is favored for the following III-V deposition. However, the low substrate temperature might induce the degradation of crystallinity simultaneously which will be investigated by the following XRD and TEM measurements.

The XRD reciprocal space mappings (RSM) were conducted to investigate the effect of substrate temperature on the crystallinity of the Ge films. **Figure 8** shows the (004) RSM of the Ge films deposited at (a) 300°C, (b) 400°C, and (c) 500°C. **Figure 8(a)** demonstrates that the Ge

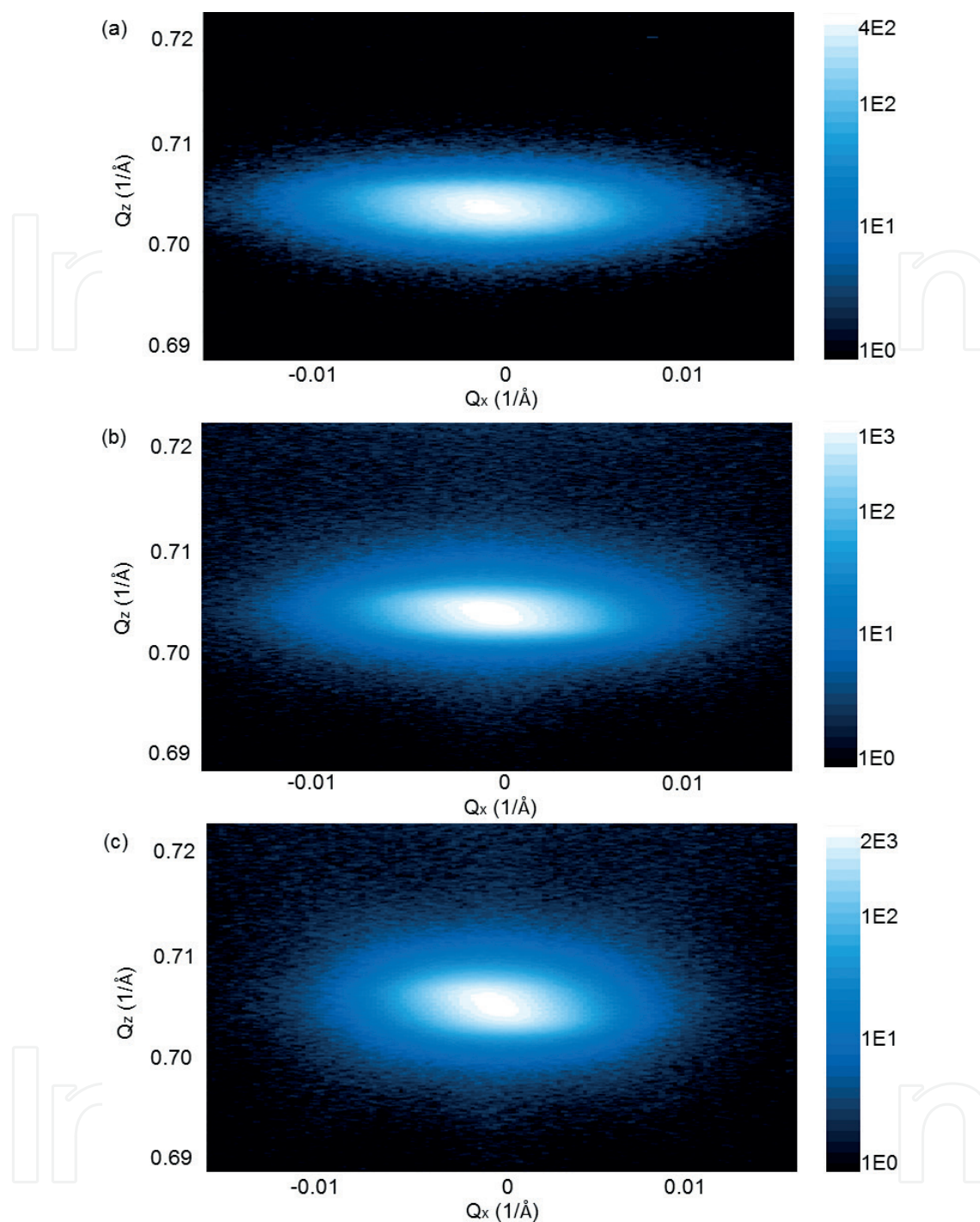


Figure 8. XRD (004) reciprocal space maps of the Ge films deposited at (a) 300°C, (b) 400°C, and (c) 500°C.

diffraction spots are elongated along the Q_x direction, which is due to the deteriorated crystal quality [35]. With the substrate temperature increasing from 300 to 500°C, the Ge peak exhibits steeper decay in the Q_x direction and the Ge peak position shows a slight upwards shift along the Q_z direction. These results indicate that the Ge film deposited at higher temperature has lower defect density and reduced compressive strain.

Micro-Raman spectra were used to investigate the structural property of the surface layer in the Ge samples deposited on Si at 300°C, 400°C, and 500°C. The penetration depth of the laser in

the Ge layer was limited within the top 20 nanometers by using the wavelength of 514 nm excitation source [36]. As shown in **Figure 9**, the Ge films exhibit peaks centered around 300 cm^{-1} corresponding to the Ge-Ge optical vibration modes [37]. All the Ge films deposited at various temperatures exhibit peaks positioned at a higher wavenumber than the bulk unstrained Ge, suggesting compressive strains in the films. With increasing substrate temperatures, the peak positions of the Ge films shift to lower wavenumbers toward that of the bulk Ge indicating decreased compressive strain in the films [38], which is in agreement with the XRD results.

The reduction of compressive strain with increasing substrate temperature might be due to the difference in linear thermal expansion coefficients between Si and Ge. The thermal expansion coefficient of Ge is $\Delta a/a(\text{Ge}) = 5.8 \times 10^{-6} \Delta T (\text{°C})$, which is larger than that of Si, $\Delta a/a(\text{Si}) = 2.6 \times 10^{-6} \Delta T (\text{°C})$ [39]. The Ge films, which are nearly fully lattice-matched to the Si substrate at the growth temperature experience tensile strain when cooling to room temperature [40]. This is because the perpendicular lattice parameter of the Ge films shrinks more easily during cooling process than the in-plane lattice which is influenced by the underneath Si substrate with lower thermal expansion coefficient.

Figure 10 shows the cross-sectional TEM images of Ge samples deposited at 300°C in (a) bright and (b) dark field, deposited at 400°C in (c) bright and (d) dark field, and deposited at 500°C in (e) bright and (f) dark field. As shown in **Figure 10(a)** and (b), the Ge film deposited at 300°C exhibits very high TDD which is estimated to be of the order of 10^{10} cm^{-2} . The high TDD might be owing to the reduced diffusion length of Ge at low temperature. With increasing substrate temperature, the TDD decreases and some planar defects are observed in the Ge film deposited at 500°C as shown in **Figure 10(c)–(f)**. The density of the planar defects is particularly high in the vicinity area of the Ge/Si interface and most of them are restricted to that region and do not extend to the film

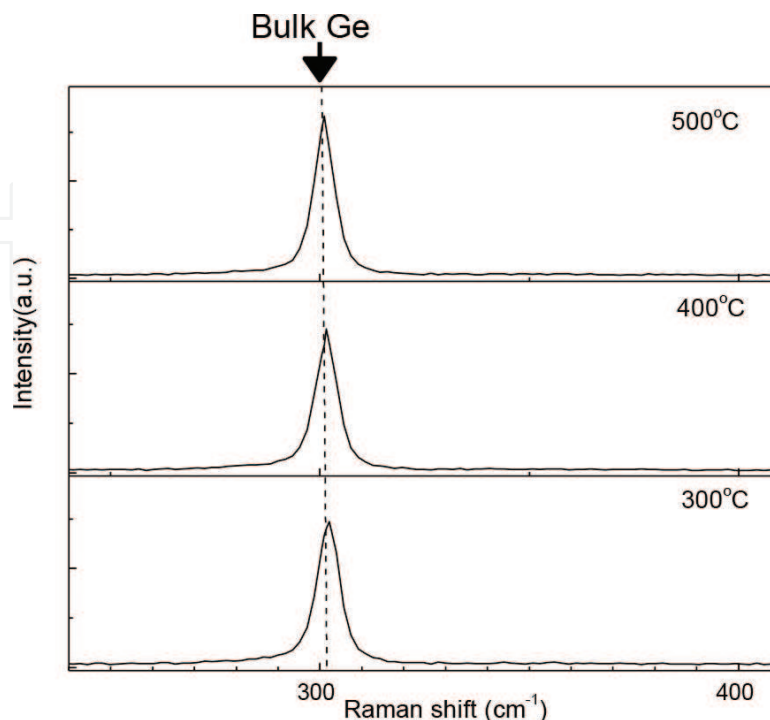


Figure 9. Raman spectra of the Ge films deposited on Si at 300, 400, and 500°C .

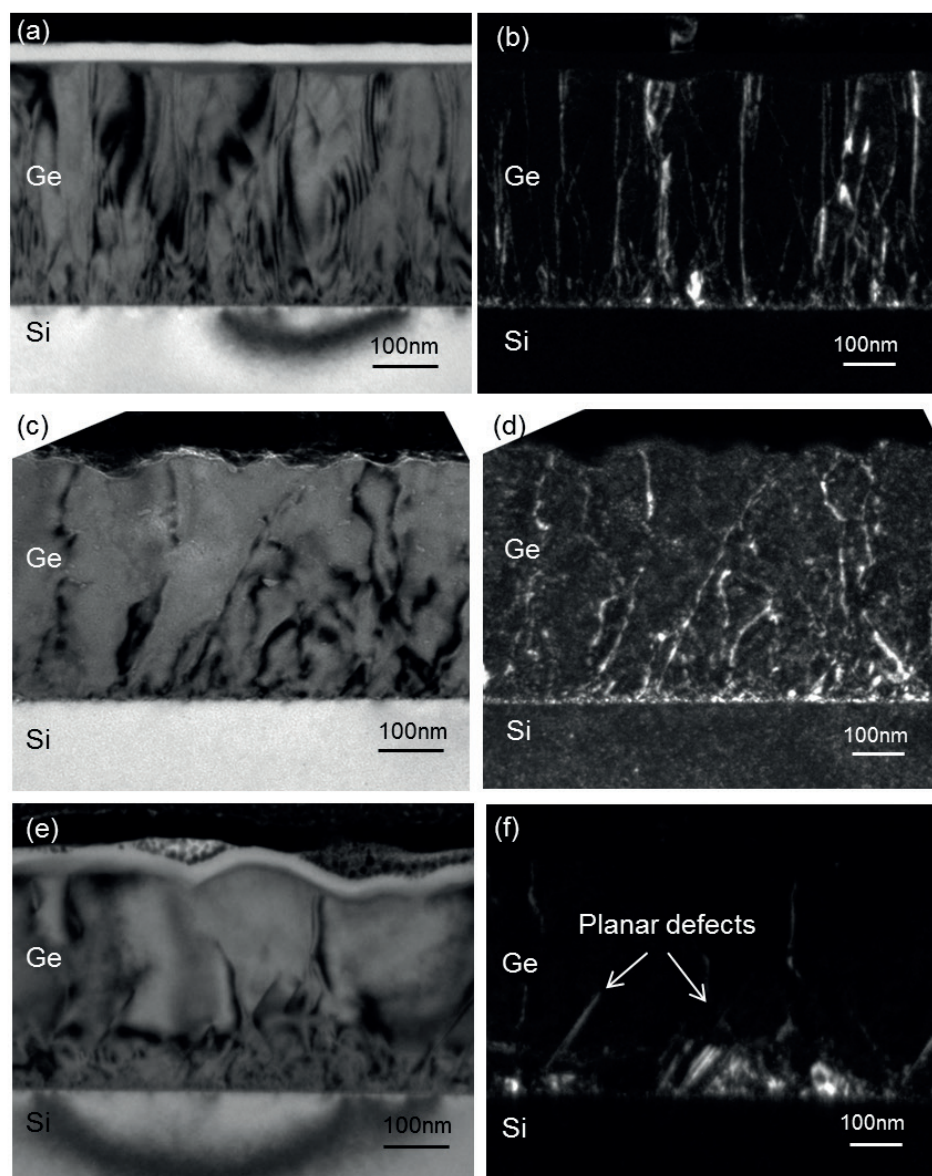


Figure 10. Cross-sectional TEM images of Ge samples deposited at 300°C in (a) bright and (b) dark field, deposited at 400°C in (c) bright and (d) dark field, and deposited at 500°C in (e) bright and (f) dark field.

surface which is consistent with previous report [41]. The TDD of the Ge film deposited at 500°C is in the order of 10^9 cm^{-2} , one magnitude order lower than that deposited at 300°C. The improved crystallinity with increasing substrate temperature agrees well with the XRD results.

5. Epitaxial growth of Ge on Si at low temperatures by one-step aluminum-assisted crystallization

The aluminum-induced crystallization (AIC) of Si, Ge and SiGe on foreign substrates has been extensively studied by several groups to obtain polycrystalline material at a low temperature [42–45]. The a-Ge/Al/c-Si structure has been investigated and epitaxial SiGe alloys

were obtained [46]. The aforementioned conventional AIC includes two steps: (1) depositing a stacked Al and amorphous Ge layer on the Si substrate, (2) postdeposition annealing to induce the layer exchange process. The postdeposition annealing introduces the diffusion of Si into the Ge layer resulting in formation of $\text{Si}_x\text{Ge}_{1-x}$ alloy. In order to achieve epitaxial growth of pure Ge on Si through Al at low temperature, one-step aluminum-assisted crystallization is developed.

The novelty of one-step aluminum-assisted crystallization of Ge epitaxy on Si lies in the elimination of the postdeposition annealing step [47]. This process simply requires sequential depositions of Al and Ge films via magnetron sputtering in the same chamber without breaking the vacuum. By applying an *in-situ* low temperature (50–150°C) heat treatment in between Al and Ge sputter depositions, the epitaxial growth of Ge on Si is achieved. This low temperature process has a low thermal budget and can fabricate pure Ge layer compared with $\text{Si}_x\text{Ge}_{1-x}$ alloy as obtained in the conventional process. The effects of Al heating temperature on the properties of the epitaxial Ge films are investigated and the mechanism of epitaxial growth of Ge on Si by one-step aluminum-assisted crystallization is discussed based on observations on samples with various Ge deposition times.

The Al films were sputter-deposited onto Si substrates at room temperature using a 2 inch intrinsic Al target (99.999% purity) at a deposition rate of 3 nm/min. The samples then underwent an *in-situ* heat treatment for 10 minutes prior to the Ge deposition. The Ge films were then sputter-deposited using a 4 inch intrinsic Ge target (99.999% purity) without further intentional substrate heating at 5 nm/min. The Al heating temperatures were varied at 50°C (Sample ID: 60-50-12), 100°C (Sample ID: 60-100-12), and 150°C (Sample ID: 60-150-12) with Al thickness of 60 nm and Ge deposition time of 12 min to investigate the effect of heating temperature. One control sample (Sample ID: 60-NA-12) did not undergo this heat treatment. Shorter Ge deposition of 1 minute (Sample ID: 60-100-1) and 3 minutes (Sample ID: 60-100-3) were experimented on substrates with 60 nm Al deposition and 100°C heat treatment as well with the aim to investigate the mechanism of Ge epitaxial growth on Si by one-step aluminum-assisted crystallization. The Ge samples were analyzed by XRD, TEM and EDS (Phillips CM200 microscope equipped with an EDAX energy dispersive X-ray spectroscopy system) measurements.

5.1. Effects of heating temperature

Figure 11(a) shows the XRD 2θ - Ω diffraction patterns of samples 60-NA-12, 60-50-12, 60-00-12 and 60-150-12. For sample 60-NA-12, the XRD pattern shows a peak at 65.2° corresponding to Al (220) and a strong Si (400) peak at 69.2° from the Si substrate. The Ge film on 60-NA-12 is amorphous due to the absence of a Ge peak. For samples 60-50-12, 60-100-12 and 60-150-12, apart from the Al peak and Si peak, a peak located at 66° is present which corresponds to Ge (400). The absence of any other Ge peaks and the results of X-ray Phi scans indicate the Ge films are single-crystalline Ge (100). **Figure 11(b)** shows the Si (220) and Ge (220) Phi scan patterns collected from sample 60-100-12 by rotating the specimen with respect to the [110] axis. The four (220) reflections are observed in the Ge Phi scan pattern which suggests the film is with fourfold symmetry about an axis normal to the Si substrate [33]. In addition, the Ge (220) reflections align with the Si substrate (220) reflections indicating the Ge is single-crystalline epitaxy film.

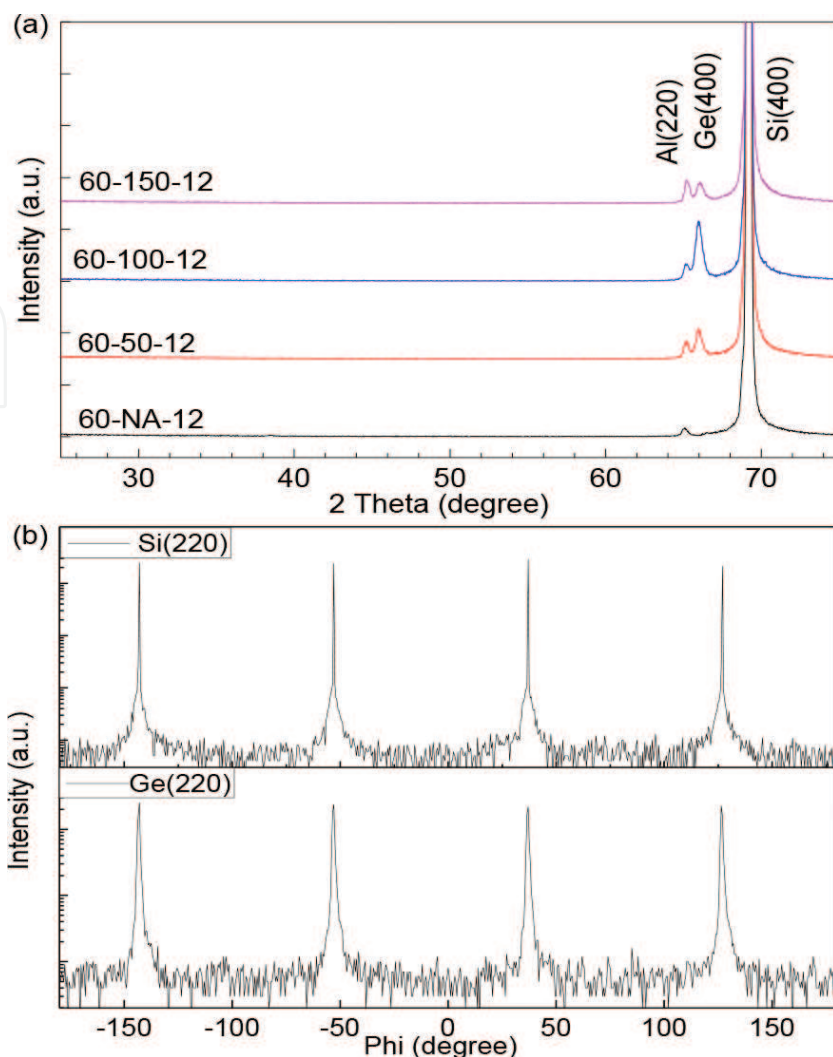


Figure 11. (a) XRD 2θ - Ω diffraction patterns of samples 60-NA-12, 60-50-12, 60-100-12 and 60-150-12, (b) Si (220) and Ge (220) phi scan patterns collected from the sample 60-100-12 showing the epitaxial relationship between the Ge film and Si substrate. (reprinted from Liu et al. [47], with the permission of AIP publishing).

The Ge peak intensity of sample 60-50-12 is lower than that of sample 60-100-12 as shown in **Figure 11(a)** due to incomplete Ge crystallization. The drop in Ge peak intensity for sample 60-150-12 might be due to the lower number of Al grain boundaries compared with that of sample 60-100-12. The Al grain boundaries play an important role in the Al-assisted crystallization process as they supply pathways for the Ge atoms to be epitaxially grown from the Si surface [46]. With increasing heating temperature, Al grain size is enlarged and therefore the density of grain boundaries is reduced [48] verified by the following TEM measurements.

Figure 12 shows the cross-sectional TEM images of samples 60-NA-12, 60-50-12, 60-100-12, and 60-150-12. **Figure 12(a)** shows the absence of Ge crystallization as the Al and amorphous Ge layers on the Si substrate. **Figure 12(b)–(d)** show the Ge epitaxial growth at selected sites on samples 60-50-12, 60-100-12, and 60-150-12. With increasing heating temperature, the crystallization sites decrease probably due to the decrease in density of Al grain boundaries [48], which

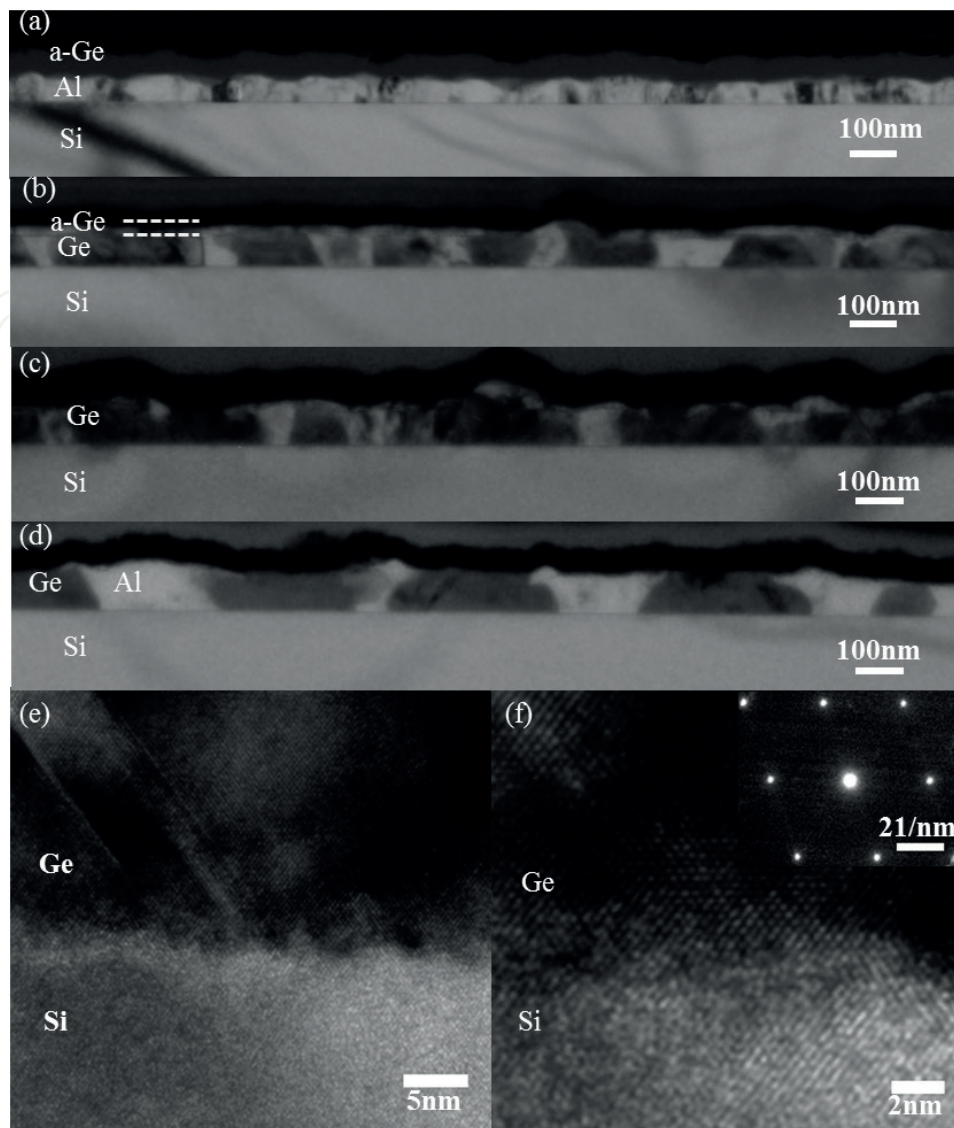


Figure 12. Cross-sectional TEM images of samples (a) 60-NA-12, (b) 60-50-12, (c) 60-100-12, and (d) 60-150-12. (e) Higher magnification and (f) atomic resolution (with SAED pattern in the insert) images of Ge/Si interface on sample 60-100-12. (reprinted from Liu et al. [47], with the permission of AIP Publishing).

are responsible for supplying pathways for the nucleation of the Ge from the Si substrate [46]. An amorphous Ge layer is shown in **Figure 12(b)** verifying the previous observations that Ge crystallization is incomplete on sample 60-50-12. Although sample 60-50-12 has more nucleation sites, it exhibits more discontinuous Ge layer compared with sample 60-100-12 owing to the incomplete crystallization.

The Ge/Si interface of sample 60-100-12 is magnified and shown in **Figure 12(e)**. The epitaxial growth of the Ge layer on Si is revealed and planar defects are observed at the interface in **Figure 12(e)**. **Figure 12(f)** shows the continuous alignment of the atoms from the Si substrate to the grown Ge film suggesting successful epitaxy. Furthermore, the electron diffraction pattern taken from the Ge layer shown in the insert to **Figure 12(f)** indicates the Ge is single crystal [49]. This result is in good agreement with the XRD measurements.

5.2. Mechanism of one-step aluminum-assisted crystallization

To better understand the mechanism of the epitaxial growth of Ge on Si through one-step aluminum-assisted crystallization, EDS mapping of samples that underwent different Ge deposition times (1 minute, 3 minutes and 12 minutes) were carried out. The cross-sectional TEM images (top row), EDS maps of Ge (middle row) and EDS maps of Al (bottom row) of samples 60-100-1, 60-100-3, and 60-100-12 are shown in **Figure 13(a)–(c)**, respectively. They reveal the Ge and Al distributions at different stages of the crystallization process. As shown, the process begins with the Ge nucleating at selected sites at the Si and Al interface. With increasing deposition time, the Ge tends to grow upwards at the initial stage and then grow laterally.

The mechanism of the epitaxial growth of Ge on Si by one-step aluminum-assisted crystallization is discussed as follows. The covalent bonds of Ge are weakened at the interface with the Al layer as a consequence of a screening effect of the free electrons in the Al layer [50]. These Ge atoms have relatively high mobility and may provide the agent for initiating the crystallization process. These mobile atoms tend to lower the Gibbs energy of the system by diffusing to sites of low energy such as the Al grain boundaries. This diffusion is sometimes called grain boundary wetting that reduces total interface energy by replacing the grain

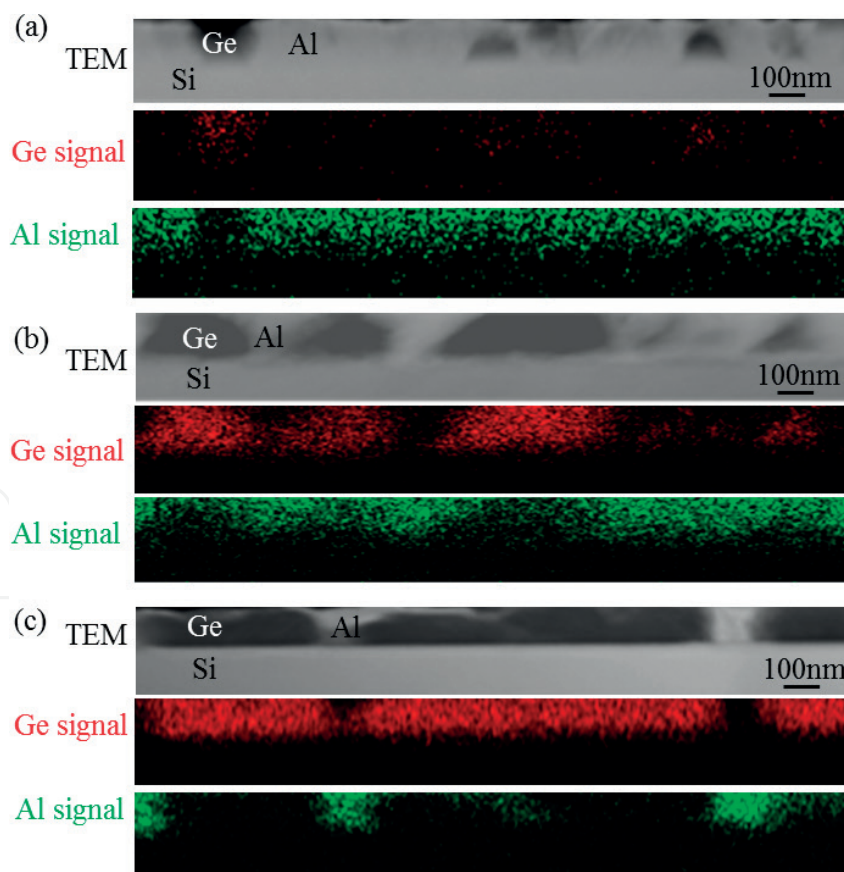


Figure 13. Cross-sectional TEM images (top), EDS maps of Ge (middle) and Al (bottom) of samples (a) 60-100-1, (b) 60-100-3, and (c) 60-100-12. (reprinted from Liu et al. [47], with the permission of AIP publishing.)

boundary with two interphase boundaries [51]. The diffusion of Ge into the Al grain boundaries forms a pathway to supply the material for crystallization. The crystallization is then driven by the reduction in bulk Gibbs energy when the material changes from amorphous to crystalline [52]. However, this can be counteracted by the increase in interface energy as crystallization proceeds [53]. When a heat treatment is applied, the interface energy at the crystalline-amorphous interface increases, while the interface energy at the crystalline-crystalline decreases [43]. This effectively reduces the energy difference between the crystalline-amorphous and the crystalline-crystalline interfaces favoring the crystallization process. This explains the observed Ge crystallization in the heat treated samples. As studied and discussed in previous work [46], the Al/Si is the preferred interface to Ge/Al for nucleation, as observed on sample 60-100-1 in this work. After the nucleation on Si substrate, the epitaxial growth of Ge continues with further incorporation of Ge atoms through the Al grain boundaries.

6. Conclusions

Epitaxial growth of Ge films on Si has been achieved using magnetron sputtering which is low cost, safe and scalable. The effects of substrate temperature on the properties of the Ge films have been investigated. The surface roughness of the Ge films increases with substrate temperature. Smooth surface with RMS roughness of 0.48 nm can be obtained at 300°C owing to the reduced diffusion length of Ge atoms at low temperature. On the other hand, the crystallinity of the Ge films could be improved by increasing substrate temperature as revealed by XRD and TEM measurements. In addition, the compressive strain in the Ge films decreases with increasing substrate temperature owing to the difference in the thermal expansion coefficients between Si and Ge.

Epitaxial growth of Ge films on Si by magnetron sputtering at low temperature has been achieved through one-step aluminum-assisted crystallization. By applying an *in-situ* low temperature (50–150°C) heat treatment in between Al and Ge sputter depositions, the epitaxial growth of Ge on Si can be achieved as verified by high resolution TEM and XRD analyses. The mechanism of epitaxial growth of Ge on Si substrate by one-step aluminum-assisted crystallization is discussed based on observations on samples with various Ge deposition times. This method significantly lowers the required temperature for and therefore the cost of epitaxial growth of Ge on Si.

Acknowledgements

This work has been supported by the Australian Government through the Australian Research Council (ARC, grant number DP160103433, LP110201112) and the Australian Renewable Energy Agency (ARENA) and by Epistar Corporation and Shin Shin Natural Gas Co., Ltd., Taiwan. Responsibility for the views, information or advice expressed herein is not accepted by the Australian Government.

Author details

Ziheng Liu*, Xiaojing Hao, Anita Ho-Baillie and Martin A. Green

*Address all correspondence to: ziheng.liu@unsw.edu.au

School of Photovoltaic and Renewable Energy Engineering, University of New South Wales, Sydney, Australia

References

- [1] Hussain AM et al. Thermal recrystallization of physical vapor deposition based germanium thin films on bulk silicon (100) physica status solidi (RRL). *Rapid Research Letters*. 2013;**7**(11):966-970
- [2] Luryi S, Kastalsky A, Bean JC. New infrared detector on a silicon chip. *Electron Devices, IEEE Transactions on*. 1984;**31**(9):1135-1139
- [3] Beeler R et al. Comparative study of InGaAs integration on bulk Ge and virtual Ge/Si substrates for low-cost photovoltaic applications. *Solar Energy Materials and Solar Cells*. 2010;**94**(12):2362-2370
- [4] King RR et al. 40% efficient metamorphic GaInP/GaInAs/Ge multijunction solar cells. *Applied Physics Letters*. 2007;**90**(18)
- [5] Guter W et al. Current-matched triple-junction solar cell reaching 41.1% conversion efficiency under concentrated sunlight. *Applied Physics Letters*. 2009;**94**(22)
- [6] Tanabe K. A review of ultrahigh efficiency III-V semiconductor compound solar cells: Multijunction tandem, lower dimensional, photonic up/down conversion and plasmonic nanometallic structures. *Energies*. 2009;**2**(3):504
- [7] Green MA. Silicon wafer-based tandem cells: The ultimate photovoltaic solution? 2014
- [8] Ringel SA et al. Single-junction InGaP/GaAs solar cells grown on Si substrates with SiGe buffer layers. *Progress in Photovoltaics: Research and Applications*. 2002;**10**(6):417-426
- [9] Roman JM. State-of-the-art of III-V solar cell fabrication technologies, device designs and applications. *Advanced Photovoltaic Cell Design*. EN548; April 27 2004
- [10] Luan H-C et al. High-quality Ge epilayers on Si with low threading-dislocation densities. *Applied Physics Letters*. 1999;**75**(19):2909-2911
- [11] Fukuda Y, Kohama Y. High quality heteroepitaxial Ge growth on (100) Si by MBE. *Journal of Crystal Growth*. 1987;**81**(1-4):451-457
- [12] Currie MT et al. Controlling threading dislocation densities in Ge on Si using graded SiGe layers and chemical-mechanical polishing. *Applied Physics Letters*. 1998;**72**(14):1718-1720

- [13] Choi D et al. Low surface roughness and threading dislocation density Ge growth on Si (001). *Journal of Crystal Growth*. 2008;**310**(18):4273-4279
- [14] Liu Z. Virtual Ge substrates for high efficiency III-V solar cells. 2014. The University of New South Wales
- [15] Frank FC, Merwe JHvd. One-dimensional dislocations. I. Static theory. *Proceedings of the Royal Society of London. Series A, Mathematical and Physical Sciences*. 1949;**198**(1053): 205-216
- [16] Volmer M, Weber A. Keimbildung in übersättigten Gebilden. *Physical Chemistry*. 1926; **119U**(1):277-301
- [17] Stranski IN, Krastanow VL, *Akad. Wiss. Lit. Mainz Math.-Natur. Kl. IIb* 1939. 146
- [18] Eaglesham DJ, Cerullo M. Dislocation-free Stranski-Krastanow growth of Ge on Si(100). *Physical Review Letters*. 1990;**64**(16):1943-1946
- [19] Mo YW et al. Kinetic pathway in Stranski-Krastanov growth of Ge on Si(001). *Physical Review Letters*. 1990;**65**(8):1020-1023
- [20] Sakai A, Tatsumi T. Defect-mediated island formation in Stranski-Krastanov growth of Ge on Si(001). *Physical Review Letters*. 1993;**71**(24):4007-4010
- [21] Sieg RM et al. Anti-phase domain-free growth of GaAs on offcut (001) Ge wafers by molecular beam epitaxy with suppressed Ge outdiffusion. *Journal of Electronic Materials*. 1998;**27**(7):900-907
- [22] Ringel SM et al. Toward achieving efficient III-V space cells on Ge/GeSi/Si wafers. *Proceedings of the second world conference and exhibition on photovoltaic solar. Energy Conversion*. 1998
- [23] Voigtländer B et al. Modification of growth kinetics in surfactant-mediated epitaxy. *Physical Review B*. 1995;**51**(12):7583-7591
- [24] Sakai A, Tatsumi T. Ge growth on Si using atomic hydrogen as a surfactant. *Applied Physics Letters*. 1994;**64**(1):52-54
- [25] Copel M et al. Influence of surfactants in Ge and Si epitaxy on Si(001). *Physical Review B*. 1990;**42**(18):11682-11689
- [26] Bean JC et al. Pseudomorphic growth of $\text{Ge}_x\text{Si}_{1-x}$ on silicon by molecular beam epitaxy. *Applied Physics Letters*. 1984;**44**(1):102-104
- [27] Eaglesham DJ, Cerullo M. Low-temperature growth of Ge on Si(100). *Applied Physics Letters*. 1991;**58**(20):2276-2278
- [28] Wietler TF, Bugiel E, Hofmann KR. Surfactant-mediated epitaxy of relaxed low-doped Ge films on Si(001) with low defect densities. *Applied Physics Letters*. 2005;**87**(18) 182102
- [29] People R, Bean JC. Calculation of critical layer thickness versus lattice mismatch for $\text{Ge}_x\text{Si}_{1-x}/\text{Si}$ strained-layer heterostructures. *Applied Physics Letters*. 1985;**47**(3):322-324

- [30] Nayfeh, A. Heteroepitaxial Growth of Relaxed Germanium on Silicon. PhD thesis Stanford University, 2006
- [31] Ferrari C, Rossetto G, Fitzgerald EA. Misfit dislocation and threading dislocation distributions in InGaAs and GeSi/Si partially relaxed heterostructures. *Materials Science and Engineering: B*. 2002;**91-92**(0):437-440
- [32] Kern W. The evolution of silicon wafer cleaning technology. *Journal of the Electrochemical Society*. 1990;**137**(6):1887-1892
- [33] Gilbert SR et al. Epitaxial growth of SrTiO₃ thin films by metalorganic chemical vapor deposition. *Applied Physics Letters*. 1995;**66**(24):3298-3300
- [34] Greene JE. Epitaxial crystal growth by sputter deposition: Applications to semiconductors. Part 2. *Critical Reviews in Solid State and Materials Sciences*. 1983;**11**(3):189-227
- [35] Yamamoto Y et al. Low threading dislocation density Ge deposited on Si (100) using RPCVD. *Solid-State Electronics*. 2011;**60**(1):2-6
- [36] Wolf ID. Micro-Raman spectroscopy to study local mechanical stress in silicon integrated circuits. *Semiconductor Science and Technology*. 1996;**11**(2):139
- [37] Loh TH et al. Ultrathin low temperature SiGe buffer for the growth of high quality Ge epilayer on Si(100) by ultrahigh vacuum chemical vapor deposition. *Applied Physics Letters*. 2007;**90**(9)
- [38] Oda K et al. Improvement of crystallinity by post-annealing and regrowth of Ge layers on Si substrates. *Thin Solid Films*. 2014;**550**(0):509-514
- [39] Sze SM. *Physics of Semiconductor Devices*. 2nd ed. New York: John Wiley and Sons; 1981
- [40] Hartmann JM et al. Reduced pressure-chemical vapor deposition of Ge thick layers on Si(001) for 1.3-1.55- μm photodetection. *Journal of Applied Physics*. 2004;**95**(10):5905-5913
- [41] Ernst F, Pirouz P. Formation of planar defects in the epitaxial growth of GaP on Si substrate by metal organic chemical-vapor deposition. *Journal of Applied Physics*. 1988;**64**(9):4526-4530
- [42] Nast O et al. Aluminum-induced crystallization of amorphous silicon on glass substrates above and below the eutectic temperature. *Applied Physics Letters*. 1998;**73**(22):3214-3216
- [43] Wang ZM et al. Thermodynamics and mechanism of metal-induced crystallization in immiscible alloy systems: Experiments and calculations on Al/a-Ge and Al/a-Si bilayers. *Physical Review B*. 2008;**77**(4):045424
- [44] Zhang T-W et al. Diffusion-controlled formation mechanism of dual-phase structure during Al induced crystallization of SiGe. *Applied Physics Letters*. 2012;**100**(7):071908
- [45] Gjukic M et al. Aluminum-induced crystallization of amorphous silicon-germanium thin films. *Applied Physics Letters*. 2004;**85**(11):2134-2136

- [46] Liu Z et al. Epitaxial growth of single-crystalline silicon–germanium on silicon by aluminium-assisted crystallization. *Scripta Materialia*. 2014;**71**(0):25-28
- [47] Liu Z et al. One-step aluminium-assisted crystallization of Ge epitaxy on Si by magnetron sputtering. *Applied Physics Letters*. 2014;**104**(5) 052107
- [48] Tsuji N et al. Strength and ductility of ultrafine grained aluminum and iron produced by ARB and annealing. *Scripta Materialia*. 2002;**47**(12):893-899
- [49] Wei S-Y et al. Epitaxial growth of heavily boron-doped Si by al(B)-induced crystallisation at low temperature for back surface field manufacturing. *CrystEngComm*. 2013;**15**(9):1680-1684
- [50] Hiraki A. Low temperature reactions at Si/metal interfaces; what is going on at the interfaces? *Surface Science Reports*. 1983;**3**(7):357-412
- [51] Wang ZM et al. “Explosive” crystallisation of amorphous germanium in Ge/Al layer systems; comparison with Si/Al layer systems. *Scripta Materialia*. 2006;**55**(11):987-990
- [52] Wang Z et al. Fundamentals of metal-induced crystallization of amorphous semiconductors. *Advanced Engineering Materials*. 2009;**11**(3):131-135
- [53] Benedictus R, Böttger A, Mittemeijer EJ. Thermodynamic model for solid-state amorphization in binary systems at interfaces and grain boundaries. *Physical Review B*. 1996;**54**(13):9109-9125

IntechOpen

